This is a repository copy of *Systems biology and metabolic modelling unveils limitations to polyhydroxybutyrate accumulation in sugarcane leaves; lessons for C4 engineering*.

Systems biology and metabolic modelling unveils limitations to polyhydroxybutyrate accumulation in sugarcane leaves; lessons for C4 engineering

Journal:	*Plant Biotechnology Journal*
Manuscript ID:	Draft
Manuscript Type:	Research Article
Date Submitted by the Author:	n/a
Complete List of Authors:	McQualter, Richard; The University of Queensland, Australian Institute of Bioengineering and Nanotechnology Bellasio, Chandra; University of Sheffield, Animal and Plant Sciences Gebbie, Leigh; Queensland University of Technology, Science and Engineering Petrasovits, Lars; The University of Queensland, Australian Institute of Bioengineering and Nanotechnology Palfreyman, Robin; The University of Queensland, Australian Institute of Bioengineering and Nanotechnology Hodson, Mark; The University of Queensland, Australian Institute of Bioengineering and Nanotechnology Plan, Manuel; The University of Queensland, Australian Institute of Bioengineering and Nanotechnology Blackman, Deborah; The University of Queensland, Australian Institute of Bioengineering and Nanotechnology Brumbley, Stevens; University of North Texas, Department of Biological Sciences Nielsen, Lars; The University of Queensland, Department of Chemical Engineering
Keywords:	photosynthesis, polyhydroxybutyrate, biopolymer, diurnal, C4 metabolic model

SCHOLARONE™
Manuscripts

1 *Full title:*

2   Systems biology and metabolic modelling unveils limitations to polyhydroxybutyrate

3 accumulation in sugarcane leaves; lessons for C$_4$ engineering.

4 *Authors full names*

5   Richard B McQualter[1,4]*   Richard.Mcqualter@unt.edu

6   Chandra Bellasio[2]*   c.bellasio@sheffield.ac.uk

7   Leigh K Gebbie[1,5]   leigh.gebbie@qut.edu.au

8   Lars A Petrasovits[1]   lapetrasovits@bigpond.com

9   Robin W Palfreyman[1]   r.palfreyman@uq.edu.au

10   Mark P Hodson[3]   m.hodson1@uq.edu.au

11   Manuel R Plan[3]   m.plan@uq.edu.au

12   Deborah M Blackman[1]   deborah.blackman@yahoo.com.au

13   Stevens M Brumbley[1,4]   sbrumbley@unt.edu

14   Lars K Nielsen[1]   lars.nielsen@uq.edu.au

15 *Institution addresses*

16   [1]Australian Institute for Bioengineering and Nanotechnology, the University of

17 Queensland, Brisbane, Qld 4072, Australia.

18   [2]Department of Animal and Plant Sciences, University of Sheffield, Western Bank,

19 Sheffield S10 2TN (UK).

20   [3]Metabolomics Australia Queensland Node, Australian Institute for Bioengineering and

21 Nanotechnology, the University of Queensland, Brisbane, QLD 4072, Australia.

22   [4]Current address: University of North Texas, Department of Biological Sciences, 1155

23 Union Circle #305220, Life Sciences Bldg A254, Denton, TX 76203-5017 USA

24   [5]Current address: QUT Science and Engineering Faculty, GPO Box 2434, Brisbane QLD

25 4001.

26

27 *These two authors contributed equally to the paper

28 *Corresponding Author*

1 Name: Richard B. McQualter

2 Address: Australian Institute for Bioengineering and Nanotechnology, Corner College and

3 Cooper Rds (Bldg 75), The University of Queensland, Brisbane Qld 4072, Australia.

4 Telephone number: +61 4 1876 0400

5 Email address: Richard.Mcqualter@unt.edu

6 *Running title:*

7 Limitations to PHB accumulation in sugarcane

8 *Keywords (6):*

9 polyhydroxybutyrate, biopolymer, diurnal, C_4 metabolic model, photosynthesis, mRNA.

10 *Word count (7000 limit):* 6822

11

Summary

In *planta* production of the bioplastic polyhydroxybutyrate (PHB) is one important way in which plant biotechnology can address environmental problems and emerging issues related to peak oil. However, high biomass C_4 plants such as maize, switch grass and sugarcane develop adverse phenotypes including stunting, chlorosis and reduced biomass as PHB levels in leaves increase. In this paper we explore limitations to PHB accumulation in sugarcane chloroplasts using a Systems Biology approach, coupled with a metabolic model of C_4 photosynthesis. Decreased assimilation was evident in high PHB-producing sugarcane plants, which also showed a dramatic decrease in sucrose and starch content of leaves. A subtle decrease in the C/N ratio was found which was not associated with a decrease in total protein content. An increase in amino acids used for nitrogen recapture was also observed. Based on the accumulation of substrates of ATP-dependent reactions we hypothesised ATP starvation in bundle sheath chloroplasts. This was supported by mRNA differential expression patterns. The disruption in ATP supply in bundle sheath cells appears to be linked to the physical presence of the PHB polymer which may disrupt photosynthesis by scattering photosynthetically active radiation and/or physically disrupting thylakoid membranes.

Introduction

Plant biotechnology plays an important role in addressing emerging issues related to climate change (Karaba et al., 2007; Varshney et al., 2011), global food security, the management of pests and diseases, and as a source of renewable feed stocks for industry (Fesenko and Edwards, 2014). While the potential to use plant biotechnology to reshape agriculture or grow renewable raw materials for industry is significant, redesigning plants using biotechnology requires detailed understanding of the plant's metabolic, gene regulatory and cell signalling pathways (Zurbriggen et al., 2012). For example, the stimulation of demand must be tuned both spatially and temporally to avoid conflict with native metabolic processes and particularly with the energy status of the cell (Morandini, 2013). Systems biology offers invaluable tools to understand emergent properties of cell biochemistry and physiology (Smolke and Silver, 2011) and is used extensively in basic research (Bellasio and Griffiths, 2014; Pick et al., 2011; Van Norman and Benfey, 2009; Zhu et al., 2010). However, the potential for understanding the effects of introduced pathways on native metabolic processes in plants has not been exploited.

In this paper we apply systems biology to study the limitations to production of the bioplastic PHB in sugarcane leaves. PHB is a thermoplastic biodegradable polymer highly valuable for medical and food packaging applications (Philip et al., 2007). Although the main PHB source is microbial fermentation, recent studies have manipulated maize, sugarcane and switchgrass for PHB production (McQualter et al., 2014a; Petrasovits et al., 2007; Petrasovits et al., 2012; Poirier and Gruys, 2001; Purnell et al., 2007; Somleva et al., 2012; Somleva et al., 2013; Somleva et al., 2008). Sugarcane is ideal for PHB production. Firstly, it accumulates huge biomass due to the high yield potential of NADP-ME C_4 photosynthesis (Sage et al., 2013), a biochemical 'turbocharger' which concentrates CO_2 around Rubisco in the bundle sheath (BS) thus suppressing photorespiration (see top half of Figure 1). Secondly, established infrastructure exists for its cultivation, harvesting, transportation and processing (Altpeter et al., 2014; Lakshmanan et al., 2005; Ming et al., 2006; Nel, 2010; Pan, 2012). And thirdly, PHB has been targeted to leaves to valorise a by-product which is generally left on the field (Landell et al., 2013).

PHB is synthesised by a three enzyme pathway and utilises acetyl-CoA as the initial substrate (Figure 1 and Supporting Table S1). A β-ketothiolase (EC 2.3.1.16) condenses two acetyl-CoA to form acetoacetyl-CoA. Acetoacetyl-CoA reductase (EC 1.1.1.36) then catalyses the formation of 3-hydroxybutyral-CoA from acetoacetyl-CoA with the aid of

NADPH. Finally, PHB synthase polymerises 3-hydroxybutyral-CoA monomers to form

PHB. The PHB biosynthesis pathway from *Cupriavidus necator* was targeted to chloroplasts

which contain abundant acetyl-CoA, ATP and reducing power. Acetyl-CoA is produced via

the lower portion of the glycolytic pathway from 3-phosphoglycerate (PGA) with the net

evolution of two CO_2, two ATP and one NADH (Supporting Table S1), PGA regeneration

through CO_2 fixation, and the re-fixation of evolved CO_2 require considerable amounts of

ATP and NADPH (Figure 1). Because of this contrast, comparing the overall effect of PHB

production with native photosynthesis is not straightforward.

Our previous studies showed that low PHB-producing sugarcane plants are phenotypically

normal. However a decrease in biomass, increased chlorosis (Petrasovits et al., 2012) or

decreased carbohydrate content occurs (McQualter et al., 2014a) as PHB accumulates beyond

a certain tipping point. This effect is reminiscent of carbon starvation (Basset et al., 2002;

Brouquisse et al., 1992; Brouquisse et al., 1991; Devaux et al., 2003; Dieuaide-Noubhani et

al., 1997; Gibon et al., 2009; James et al., 1996; Schluter et al., 2013; Schluter et al., 2012)

and could be directly due to excessive diversion of carbon and energy to support PHB

synthesis. Here we studied various indicators of carbon starvation including total protein

content and the carbon/nitrogen ratio (Gibon et al., 2009). We resolved the temporal

dynamics of 48 metabolites, including carbohydrates and amino acids, at seven sampling time

points throughout the light/dark cycle. A metabolic model was newly designed starting from

Bellasio and Griffiths (2014) to incorporate effects of PHB synthesis on native metabolism.

Further, the metabolic model predicted changes in ATP and NADPH demand associated with

the allocation of PHB synthesis to mesophyll (M) or bundle sheath (BS). The model

predictions were further supported by comparative transcriptomic data obtained by next

generation sequencing. We found that minor carbon starvation was evident, but not directly

due to excessive diversion of carbon and energy to support PHB synthesis. The evidence

suggests that the physical presence of PHB granules perturbs ATP production in BS.

Results

Photosynthetic assimilation rate

While the cause of chlorosis and decreased biomass in high PHB producing plants is unknown, it has been speculated that the photosynthetic efficiency of these plants is compromised (Somleva et al., 2013).To determine whether the stunted phenotype displayed by high PHB-producing lines (McQualter et al., 2014b) might be linked to changes in net assimilation (*A*) we compared a range of four month old, glasshouse grown PHB-producing lines across the threshold at which carbohydrate becomes significantly depleted. These included sugarcane WT cultivar Q117 and transgenic PHB-producing lines with increasing PHB production levels in leaves [individually reported in Figure 2 caption (Petrasovits et al., 2012)]. *A* in lines TA4 and 4F1 (*A*=18.7±1.5 and 19.1±1.8 $\mu mol \cdot m^{-2} \cdot s^{-1}$ respectively) was comparable to WT (16.7±2.9 $\mu mol \cdot m^{-2} \cdot s^{-1}$, Figure 2). For the highest PHB-producing lines 8C8 and 7C3 however, *A* was much lower than WT (12.4±1.3 and 6.1±1.7 $\mu mol \cdot m^{-2} \cdot s^{-1}$ respectively, Figure 2).

Carbon / nitrogen balance

Diversion of carbon into a non-reusable PHB sink could potentially lead a situation known as carbon starvation. Symptoms of carbon starvation include reduced C/N, increased proteolysis and changes in amino acid composition. We measured carbon and nitrogen content in the leaves of our PHB producing plants. Leaf material for this and subsequent analyses came from plants grown in a plant growth chamber with controlled lighting and temperature. Total carbon content was unaffected by the introduction of the PHB metabolic sink at PHB levels of around 1-1.5% leaf DW, with no chlorosis or stunting (Figure 3A), however a slight increase in total N was observed (Figure 3B) which subtly decreased the C/N ratio in PHB lines (Figure 3C). Protein content was not significantly different between WT and the transgenic lines (Figure 3D). Overall these results suggest mild carbon starvation. To disentangle possible contrasting trends, we then resolved individual C and N metabolites over seven sampling points in a diurnal cycle (Figure 4 and S1).

Changes in metabolites across the diurnal cycle.

Starch and sucrose accumulation rates were estimated as the difference between their abundance at onset of light and end of light, divided by hours of light. For starch the rate of accumulation was 42, 6 and 10 mg$\cdot$100$^{-1}\cdot$g^{-1}leaf DW$\cdot$hr^{-1} respectively for WT, 7B4 and 7C3. For sucrose the rate of accumulation was 161, 67 and 62 mg$\cdot$100$^{-1}\cdot$g^{-1}leaf DW$\cdot$hr^{-1} for WT, 7B4 and 7C3 respectively. The precursor of sucrose, uridine diphosphoglucose (UDPG) did not vary appreciably between WT and PHB-producing lines, suggesting that sucrose synthesis may have been regulated at another stage, perhaps at the level of sugar phosphates synthesis. While in WT sugar phosphates increased during the light and decreased in the dark (Geiger and Servaites, 1994; Weise et al., 2011), in PHB-producing lines G6P and F6P accumulated in the dark. Accumulation of G6P and F6P was accompanied by a dramatic three-fold higher accumulation of Ribose-5P and Ribulose-5P during the light (Figure 4) in PHB-producing lines compared to WT. This suggests that perhaps the regeneration of ADP-glucose and RuBP, reactions requiring ATP, were down-regulated. We hypothesised that PHB synthesis in BS reduced ATP availability therein. Metabolic modelling (Bellasio and Griffiths, 2014) has previously clarified that this situation would create a bottleneck in carbon assimilation and bring about a reduction in NADPH demand in BS (see Discussion). This hypothesis is consistent with observed increases in low energy metabolites ADP and AMP in PHB-producing lines (Figure 4). Further, in the PHB-producing lines, malate, the key carrier of reducing power to BS was more abundant (Figure 4), suggesting lower NADPH demand in BS. In this situation, to operate a functional C_4 cycle, CO_2 delivery to BS would be shifted from the malate/pyruvate shuttle to the aspartate/alanine shuttle (Bellasio and Griffiths, 2014). Consistently, in the PHB-producing lines we observed an increase in aspartate and alanine and a substantial decrease in pyruvate (Figure 4).

Glutamine and glycine increased and aspartate and glutamate decreased dramatically during the first four hours of the light cycle in WT sugarcane (Figure 4). Aspartate showed a similar diurnal profile in WT and line 7B4 while in the highest PHB-producing line 7C3, aspartate was more abundant at the onset of first light. Glutamate in WT decreased to a minimum value over the first four hours of light then recovered and maintained at its original peak value for the duration of the dark period. Both 7B4 and 7C3 showed the same initial decrease in glutamate over the first four hours of light. However, during the remainder of the light period, glutamate stayed at this minimum value until end of light. The profile of glutamine was essentially the inverse of glutamate. The diurnal fluctuation in glycine levels was subdued in PHB-producing lines compared to WT. All other amino acids were either equivalent or elevated in PHB-producing lines compared to WT (Figure 4).

The combined abundance of citrate and isocitrate, metabolites of the tricarboxylic acid (TCA) cycle, was lower in PHB-producing lines than in WT (Figure 4). Aconitate content was elevated in PHB-producing lines, compared to WT, particularly so in the highest PHB-producing line 7C3. The organic acid α-ketoglutarate, which also acts as a carbon scaffold for amino acid synthesis by combining with ammonia to form glutamate (Magalhaes et al., 1974), was less abundant in PHB-producing lines than WT. Differences between scarce amounts of succinate and fumarate were difficult to determine while glyoxylate was similarly abundant in WT and PHB-producing lines.

mRNA differential expression

Of a total of 31345 genes compared, 177 were differentially expressed including 172 native genes and 5 transgenes (>2 fold difference, q< 0.05, Table S2). Of these, 91 were down-regulated and 86 (including 5 transgenes) were up-regulated in expression in the transgenic line. A subset of the differentially expressed genes from central carbon metabolism is shown in Table 1.

We explored links between transcript abundance and changes in metabolite abundance. The results suggest a major shift in carbon metabolism synthesis to degradation: i) starch synthase III-1a, involved in synthesis of amylopectin is down-regulated (Table 1). ii) beta-amylase, involved in starch degradation is up-regulated (Table 1). iii) Sucrose synthase and beta fructofuranosidase (invertase), are up-regulated (Table 1). These are cytosolic proteins involved in degrading sucrose to UDP-glucose and fructose. Further, a soluble acid invertase localized to the vacuole (Rae et al., 2011) is down-regulated (Table 1) supporting the idea of a change in the sucrose accumulation dynamics. iv) Chloroplastic phosphoglucomutase, which was up-regulated (Table 1), is a major controller of carbon exiting the reductive pentose phosphate cycle providing G1P for starch synthesis, regulated by sugar-phosphates and PGA, however, the reaction is reversible and here it could be involved in starch degradation. v) A Chloroplastic fructokinase-like protein, was strongly up-regulated (Table 1). These are potential plastidial thioredoxin z (TRX z) targets involved in sugar signalling and redox regulation of transcription of the chloroplast and shown to be involved in control of plant carbon metabolism (Arsova et al., 2010; Gilkerson et al., 2012). Phosphoenolpyruvate carboxylase kinase 1 (PPCK1, Figure 1), which activates C_4 PEPC by reversible phosphorylation, was down-regulated (Table 1). C_4 PEPC (Shenton et al., 2006) plays a key role in maintaining the C:N balance by providing of C skeletons for amino acid

biosynthesis as well as supplying malate for decarboxylation and NADPH generation in the BS. Studies in Arabidopsis and rice show that PPCK genes are supressed by Pi and induced by Pi starvation, carbon availability and increasing intracellular pH (Chen et al., 2009; Fukayama et al., 2006).

An NADP-malic enzyme (NADP-ME) transcript similar to ZmCyt3-NADP-ME, which responds to high pH in leaf and stem and abscisic acid in roots (Alvarez et al., 2013), was down-regulated in the PHB producing line. The remaining four members of the NADP-ME family, similar to ZmC4-NADP-ME, ZmnonC4-NADP-ME, Zmcyt1-NADP-ME and Zmcyt2-NADP-ME, (Alvarez et al., 2013) where unaffected.

A major shift of nitrogen metabolism from assimilation to recapturing was apparent: i) while the expression of the glutamate synthase (Fd-GOGAT) involved in nitrogen assimilation (Watanabe et al., 1996) did not change (not shown), the expression of NADH-GOGAT, involved in the utilization of remobilized nitrogen (Hayakawa et al., 1994), increased three fold (Table 1). ii) The up-regulation (Table 1) of chloroplastic glutamine synthetase (GS), which reacts glutamate and ammonia to glutamine, may act as a scavenger of the nascent ammonia resulting from increased amino acid catabolism (Sakakibara et al., 1992). iii) The gene for asparagine synthetase ASN1 is up-regulated (Table 1). Asparagine is a favoured compound for nitrogen storage and transport (Sieciechowicz et al., 1988). The expression of ASN1 is under the metabolic control of the C/N ratio (Hanson et al., 2008; Lam et al., 1994), and ASN1 was induced by stresses and repressed in the presence of sucrose or glucose (Baena-Gonzalez et al., 2007). This suggests that when C/N ratios decrease (Figure 3), N is directed into asparagine (Figure 4), which acts as a shunt for storage and/or long-distance transport of nitrogen (Lea and Miflin, 1980; Lea et al., 1990). iv) A nitrate/nitrite transporter (NRT2.5) was down-regulated (Table 1). This transporter may play a role in the transport of stored nitrate from the vacuole into the cytoplasm, and was found to be important when nitrate uptake is reduced during senescence, either sugar-regulated or related to leaf development (Okamoto et al., 2003; Orsel et al., 2004; Rossato et al., 2001). v) A nitrilase gene, similar to maize nitrilase 1, which is involved in auxin biosynthesis and/or cyanide detoxification (Kriechbaumer et al., 2007; Park et al., 2003) was down-regulated (Table 1). vi) One isoform of phenylalanine ammonia-lyase (PAL) was up-regulated (Table 1). PAL is the first and committed step in the phenyl propanoid pathway and is therefore involved in the biosynthesis of the polyphenol compounds such as flavonoids, phenylpropanoids, and lignin. It responds to stress events (Di Ferdinando et al., 2012; Fini et al., 2011), may be responsible

for ammonia release, and may be partially responsible for the up-regulation of ammonia

scavenging GS.

Metabolic modelling

To explore the possible reasons underpinning insufficient ATP supply in BS, we included

the main reactions of C_4 photosynthesis together with PHB production (Figure 1) in a

comprehensive metabolic model (Table 2, an Excel version is available in Supporting

information). Firstly we asked whether PHB synthesis constitutes a substantial ATP and

NADPH sink. In the young sugarcane plants used for the diurnal study, the leaf material

accounted for around 90% of the entire plant biomass and 0.9 g/100 g and 1.08 g/100 g of

assimilate was directed to PHB production for 7B4 and 7C3 respectively. Figure 5A and 5B

show the total ATP and NADPH demand for assimilation at increasing levels of carbon

diversion to PHB (r_{CD} is the ratio of PGA used for PHB synthesis over that reduced by the

RPP cycle). Although PHB synthesis results in net NADPH and ATP production, CO_2 is lost

in pyruvate decarboxylation (Figure 1), and the recapture of lost CO_2 is metabolically costly.

These two processes largely compensate and on a net assimilation basis PHB synthesis

results in a negligible 0.5 and 0.9% increase for ATP and NADPH demand respectively when

r_{CD} increases from 0 to 0.1 (Figure 5A and 5B).

We further interrogated the model to see whether metabolic impairment can be due to the

compartmentalisation of PHB synthesis, which mainly occurs in BS chloroplasts (McQualter

et al., 2014b; Petrasovits et al., 2012). Figure 5C shows that the relative ATP demand in BS

increased at increasing r_{CD} but only when PHB synthesis was compartmentalised to M. When

PHB synthesis was all compartmentalised to BS (V_{DBS}/V_D=1) ATP demand in BS decreased

for increasing r_{CD} reflecting the ATP advantage of pyruvate decarboxylation in BS. Figure

5D shows that the relative NADPH demand in BS decreases with PHB synthesis because of

the reducing power made available with pyruvate oxidative decarboxylation, thus confirming

that PHB synthesis does not constitute an additional burden on native metabolism.

Finally we asked whether the decreased NADPH demand in BS could bring about

increased pressure on the transamination machinery and on the aspartate/alanine CO_2 shuttle.

Indeed, model output predicted an increased transamination rate (Figure 5E) and an increased

engagement of aspartate/malate decarboxylation (Figure 5F) at increasing r_{CD} when

V_{DBS}/V_D>0.2. Note that, because we hypothesised that ATP supply is limiting in BS, the

model output shown in Figure 5 refers to the condition in which the ATP demand in BS is

minimum (Bellasio and Griffiths, 2014). Other cases are shown in Supporting Figure S2.

Discussion

In this study we applied a systems biology approach to study the limitations to PHB

accumulation in sugarcane leaves following the observed chlorosis and reduced biomass in

high PHB-producing transgenic sugarcane lines. Firstly we investigated C and N

accumulation in leaves and we could measure a decrease in C/N but no decrease in total

protein content. If these were the only results, we could have concluded that only mild carbon

starvation occurred. However, when we augmented the resolution by analysing the daily

fluctuations of 48 metabolites, we observed a dramatic decrease in sucrose and starch

accumulation dynamics, and an increase in those amino acids used for N recapture and long

distance transport. Further, from observing the dynamic accumulation of substrates of ATP

dependent reactions (e.g. RuP, R5P, F6P, AMP) we hypothesised that ATP starvation is

occurring in BS. Overall this hypothesis was confirmed by analysing mRNA differential

expression, which highlighted three patterns: i) a shift in the CCM to adjust for reduced ATP

availability in BS and consequent reduced NADPH demand; ii) a shift from carbohydrate

synthesis to degradation; iii) a shift from N assimilation to N

mobilisation/recapture/transport. Modelling highlighted that it is unlikely that carbon

starvation was triggered directly by the additional burden of PHB. Further it showed that

compartmentalisation of PHB to BS was not responsible for a change in ATP/NADPH

source/sink equilibrium.

Decreased photosynthetic assimilation rate was observed in high but not low PHB-

producers (Figure 1). Perhaps not synthesis but accumulation of PHB is responsible for

degrading photosynthetic capacity, mediated by the physical presence of polymer granules in

the chloroplast (Nawrath et al., 1994; Somleva et al., 2013). PHB granules change cell

refractivity, and influence light-scattering properties in bacteria (Srienc et al., 1984). Further,

because of space limitations, growing PHB granules compete for space with the

photosynthetic machinery and inevitably disrupt thylakoid spatial organisation (Bohmert et

al., 2000; Nawrath et al., 1994; Petrasovits et al., 2007; Petrasovits et al., 2012; Saruul et al.,

2002; Somleva et al., 2008) (Figure 6). This could reduce the ATP availability in BS below

the minimum threshold limit, under which RuBP regeneration is impaired (Bellasio and

Griffiths, 2014). In fact, there is a finite window of plasticity of C_4 metabolism: some of the

ATP demand (i.e. conversion of PGA to triose phosphates) can be shifted to M, but ATP

requirements for RuBP regeneration and the photorespiratory carbon oxidation (PCO) cycle

are supplied exclusively by ATP produced in BS (Figure 1). If photophosphorylation is

impaired because light reaching BS chloroplasts is not sufficient, the photosynthetic

machinery jams, resulting in a decreased NADPH demand in BS and limited malate

decarboxylation. This could lead to accumulation of malate and depletion of pyruvate as

observed in PHB sugarcane lines. The feedback on malate could also be at the electron

transport level: less light in BS would require less NDH-dependent cyclic electron flow in BS

and this could feedback through thioredoxin to NADP-dependent malic enzyme deactivation

(Bellasio and Griffiths, 2014; Drincovich and Andreo, 1994). In the same manner, other

enzymes which depend on thioredoxin for activation could be affected. For example, starch is

synthesised by ADP-glucose pyrophosphorylase (AGPase) which is activated by thioredoxin,

and some beta-amylases may also be redox-regulated (Baier and Dietz, 2005; Geigenberger

et al., 2005; Michalska et al., 2009; Thormahlen et al., 2013; Valerio et al., 2011). Hence, the

diminished starch production in PHB-producing sugarcane plants could be evidence of redox

regulation associated with polymer shading. Additionally, reduced light availability in BS

could be responsible for the substantial decrease in sucrose in PHB-producing sugarcane

lines. Low light intensities during the growth of rice resulted in an accumulation of fructose

2,6-bisphosphate (F26BP) (Reddy and Das, 1987) which modulates the key enzymes of

sucrose biosynthesis thus regulating carbon flow under conditions of limited photosynthesis

(Nielsen et al., 2004).

Improvement of PHB production in sugarcane

Strategies to increase PHB production in plants have relied initially on determining the

most suitable sub-cellular compartment for expression of the PHB pathway (Nawrath et al.,

1994; Petrasovits et al., 2007), with sufficient enzyme activity to maximise use of available

substrate (Bohmert-Tatarev et al., 2011; Petrasovits et al., 2012; Somleva et al., 2008).

Access to substrate in M was found to be problematic in C_4 grasses (McQualter et al., 2014b;

Petrasovits et al., 2013) and remedied by the use of an acetoacetyl-CoA synthase in place of a

β-ketothiolase (McQualter et al., 2014a). Increasing *A* by adjusting flux through the RPP

cycle (Somleva et al., 2013) significantly corrected adverse phenotypes and increased PHB

production in switchgrass plants. Enhanced *A* coupled with an inducible system for PHB

pathway gene expression (Kourtz et al., 2007) could provide further improvements. In C_4

plants there may need to be some trade-offs in PHB synthesis: excluding PHB production

from BS [for example, using the PEPC promoter (Matsuoka et al., 1994)] excludes using

20% of the photosynthetically active volume of the leaf (Hattersley, 1984) for PHB

accumulation, but this might be compensated for by a resultant increase in BS ATP and hence

A. Manipulating energy supply has not yet been considered as a strategy for enhancing PHB

production, but here we show that this may be a major consideration in C_4 plants.

Alternatively, peroxisomal PHB production, where shading or disruption of chloroplasts

should not be problematic, has shown promise and could be explored further (Tilbrook et al.,

2011; Tilbrook et al., 2014). Other sub-cellular compartments do not appear to be suitable

(Petrasovits et al., 2007; Poirier et al., 1992).

Lessons for C_4 engineering

In recent years a substantial effort has been directed towards engineering C_4 systems in C_3

plants such as rice (Kajala et al., 2011; von Caemmerer et al., 2012). Morandini (2013) stated

the importance of an integrated approach in understanding the constraints to genetic

manipulation and Driever and Kromdijk (2013) recently reviewed several potential issues

arising from manipulation of a C_3 system, with particular regard to the interaction between

reducing power requirements, redox signalling and the native C_3 metabolism. Our work in

sugarcane highlights additional engineering challenges unique to the complex C_4 anatomical-

biochemical machinery, including physical constraints such as volume and light availability,

substrate availability and the need for a functional electron transport chain to supply cofactors

NADPH and ATP. For C_4 photosynthesis to work, sufficient ATP has to be made available in

BS: this requires space for the light harvesting machinery and sufficient light to reach BS to

drive photophosphorylation. Thus, for C_4 rice, the physiology of transport between M and BS

needs to be considered. The equations for the flow between M and BS that we presented here

may be a valuable tool in this endeavour.

Conclusion

In this study we investigated why increased chlorosis and decreased carbohydrate content

and biomass occurred in transgenic PHB-producing sugarcane as PHB accumulates above a

certain level in leaf tissue. Using a systems biology approach together with a metabolic

model of C_4 photosynthesis, we were able to identify mild carbon starvation in our high PHB

producers. Modelling highlighted that ATP starvation in BS was the cause, rather than carbon

starvation triggered directly by the additional burden of PHB biosynthesis. ATP starvation in

BS is thought to be directly due to the presence of PHB granules in BS chloroplasts, which either scatter photosynthetically active radiation due to their refractive properties, or physically disrupt thylakoid membranes. The findings of this study highlight the importance of C_4 metabolic models in helping to decipher the complex data generated from this kind of study.

Materials and Methods

Plants

PHB-producing sugarcane lines TA4, 4F1, 8C8, 7B4 and 7C3, derivatives of cultivar Q117, have been described previously (Petrasovits et al., 2007) and contain genes encoding PHB biosynthesis enzymes [β-ketothiolase (PHAA), acetoacetyl-reductase (PHAB) and PHB synthase (PHAC)] under the control of the Cabm5 promoter (Sullivan et al., 1989) and targeted to plastids. Plants were propagated from single eye stem cuttings in vermiculite fertilized with osmocote (Scotts, Bella Vista, NSW, Australia) and grown under ambient and supplemental lighting in a temperature controlled glasshouse (28˚C) at the University of North Texas, Denton, Texas.

Gas exchange measurements

Gas exchange measurements were performed on glasshouse grown PHB-producing sugarcane lines TA4, 4F1, 8C8, 7C3 and WT Q117. Measurements were taken during winter with supplemental lighting, commenced at 0800 hours and lasted till midday. The youngest fully expanded three leaves, sampled from at least three different tillers per each genotype, were measured using a portable infrared-gas analyser (IRGA, LI6400 XT: Licor, Lincoln, Nebraska, USA) equipped with a 6 cm^3 leaf chamber and a 6400-02B Red Blue light. Leaves were acclimated for 2 min at a photosynthetic photon flux density and measured 3 times at 1 minute intervals (PPFD) of 1500 μmol·m^{-2}·s^{-1}, CO_2 concentration of 400 μmol·mol^{-1}, temperature of 27ºC, air flow adjusted to maintain vapour pressure deficit 1.0–1.2 kPa.

Diurnal study

Thirty single-eye stem cuttings each of WT Q117, 7B4 and 7C3 were planted into trays containing well watered vermiculite (Ausperl, Sydney, NSW, Australia) mixed with

osmocote. The cuttings were germinated and maintained in an E36-HO plant growth cabinet

(Percival Scientific, Inc. Perry, IA, USA). PPFD was set at 1250 $\mu mol \cdot m^{-2} \cdot s^{-1}$ on a 12 hour

light (28˚C), 12 dark (24˚C) cycle. At the six leaf stage, the bottom three leaves were

removed from three randomly selected replicates of each line and snap frozen in liquid N_2.

The tissue was ground to a fine powder in liquid N_2 and stored at -80°C prior to processing.

The first sampling period commenced at the end of a 12 hour period of dark and was repeated

every four hours to yield a total of seven sampling points representing a diurnal cycle of 12

hour light and 12 hour dark.

Elemental analysis

To obtain sufficient sample for analysis of total carbon and nitrogen content, some of the

ground leaf material from each of the seven diurnal time points was pooled for two replicates.

Elemental analysis was performed using a CHN elemental analyser by the Analytical

Services Unit at the School of Agriculture and Food Sciences, the University of Queensland.

Starch/PHB

Approximately 100 mg of frozen ground leaf material per sample was used for the

analysis. Starch was determined by a two-step enzymatic hydrolysis and HPLC determination

of resulting glucose according to (Sluiter and Sluiter, 2005). PHB content was determined

from 10-20 mg of dried leaf material by measuring its acid hydrolysis product, crotonic acid

by HPLC (Petrasovits *et al.*, 2007).

Metabolite extraction

Metabolites were extracted for subsequent liquid chromatography using a modification

from (Glassop et al., 2007). Briefly, 100 mg frozen leaf powder was added to 700 μl

extraction solution. The extraction solution consisted of 70 ml methanol, 200 μl of 10 mM

$^{13}C_5^{15}N$-valine (aq); 200 μl of 1 mM $^{13}C_6$-sorbitol (in MeOH); 200 μl of 5 mM 1,2-$^{13}C_2$-

myristic acid (in $CHCl_3$), 4 ml of 0.2 $mg \cdot ml^{-1}$ adonitol + 0.2 $mg \cdot ml^{-1}$ norleucine (aq), 6 ml of

2 $mg \cdot ml^{-1}$ nonadecanoate-methyl ester (in $CHCl_3$). Samples were immediately incubated at

70°C for 10 min with frequent inversion. 580 μl deionised water and 500 μl $CHCl_3$ were then

added and the sample was vortexed for 1 min. Polar and non-polar phases were separated by

centrifugation at 15,000 g for 10 min at 4°C. The polar phase was re-extracted with $CHCl_3$.

Central carbon metabolites:

Reference standards and tributylamine (puriss plus grade) were purchased from Sigma Aldrich (Sigma Aldrich, NSW, Australia). HPLC Grade acetonitrile and acetic acid (AR Grade) was purchased from RCI Labscan (Bangkok, Thailand) and Labscan (Gliwice, Poland) respectively. Deionised water was generated via an Elga Purelab Classic water purification unit (Veolia Water Solutions and Technologies, Saint Maurice Cedex, France).

Liquid chromatography tandem mass spectrometry (LC-MS/MS) data were acquired as described in Dietmair et al, 2012 with the following modifications: the analytical column was equipped with a pre-column Security Guard Gemini-NX C18 4 mm × 2 mm (Phenomenex, Aschaffenburg, Germany); the following additional analytes were quantified: cyclic AMP, glyoxylate, glycolate, creatine phosphate and UDP N-acetylglucosamine. The samples were run with sample- and analyte-relevant calibration standards and pooled quality-control samples (Sangster et al, 2006; Hodson et al, 2009) to control for reproducibility of data acquisition and to ensure data integrity. Azidothymidine (AZT) was used as an internal standard at a final concentration of 10 μM. Analyte stock solutions were prepared in purified water (Veolia) and aliquots of each solution were mixed to achieve a final calibrant solution at 200 μM. This calibrant solution was serially diluted and the dilutions used as calibration standards from 200 to 0.006 μM, constituting $9 \leq x \leq 20$ calibration points for all analytes to account for differential responses in the mass spectrometer. Data were processed and analysed in Analyst 1.5.2 and MultiQuant 2.1.1 (ABSciex, Canada).

Amino acid analysis

Amino acids were quantified with a high-throughput derivatisation-reverse phase HPLC described previously (Chacko et al., 2014; Dietmair et al., 2012; Dietmair et al., 2010). In brief, 0.5 μL of sample containing 250 μM of sarcosine and 2-aminobutanoic acid, as internal standards, was added into 2.5 μL of borate buffer (Agilent PN: 5061-3339), mixed and incubated for 20 s at 4°C. Amino acids were derivatised in two steps by a high-performance autosampler. 1 μL of OPA reagent (Agilent PN: 5061-3335) was reacted for 20 s at 4°C, then 0.4 μL of FMOC reagent (Agilent PN: 5061-3337) was added, mixed and incubated for 20s at 4°C. 45.6 μL of Buffer A (40 mM Na_2HPO_4, 0.02% NaN_3, pH 7.8) was added added to lower the pH of the reaction, then injected in an Agilent Zorbax Extend C-18 column (3.5 μm, 4.6×150 mm, Agilent PN: 763953-902) with a guard column (SecurityGuard Gemini C18, Phenomenex PN: AJO-7597) kept at 37°C . Gradient elution was performed using an

Agilent 1200-SL HPLC system, at a flow rate of 2 mL·min^{-1}. The gradient was 2-45% Buffer B (45% acetonitrile, 45% methanol and 10% water) from 0-18min, 50-60% B from 18.1-20 min, 100% B from 20.1-24 min, and 2% B from 24.1-27 min. A fluorescence detector was used to detect OPA-derivatised amino acids from 1 to 18 min at 340_{ex} and 450_{em} nm and FMOC-derivatised amino acids from 18 to 27 min at 266_{ex} and 305em nm). The samples were run with sample- and analyte-relevant calibration standards and pooled QC samples (Sangster et al, 2006; Hodson et al, 2009) to control for reproducibility of data acquisition and to ensure data integrity.

Sucrose analysis

Sucrose was quantified by ion-exclusion chromatography using an Agilent 1200 HPLC system and a Phenomenex Rezex RHM-monosaccharide H$^+$ column (8% cross-linked sulfonated styrene-divinylbenzene, 7.8×300 mm, PN: 00H-0132-K0) equipped with guard column (SecurityGuard Carbo-H, Phenomenex PN: AJO-4490) according to (Dietmair et al., 2010). Briefly, 30 µL of sample was injected using an autosampler (Agilent HiP-ALS, G1367B), column was thermostatted at 70°C (Agilent TCC, G1316A). Sucrose was eluted isocratically at 0.4 mL·min^{-1} for 21 min at 15°C with high purity water (18.2 MΩ·cm) to avoid high temperature acid hydrolysis. Sucrose was quantified using a refractive index detector (Agilent RID, G1362A) set on positive polarity and optical unit temperature of 40°C. The samples were run with sample- and analyte-relevant calibration standards and pooled quality-control samples (Sangster et al, 2006; Hodson et al, 2009) to control for reproducibility of data acquisition and to ensure data integrity.

mRNA differential expression

To provide material for mRNA differential expression analysis, WT Q117 and 7B4 were grown according to the parameters used in the diurnal study. RNA was isolated from 100 mg of frozen leaf tissue sampled from five random plants 3 hours into the light period with the Agilent RNA kit following the manufacturer's instructions. 400 µL of extract were purified on multiple columns to avoid column saturation and DNA contamination. The RNA was quantified on an Agilent Technologies 2100 Bioanalyzer following the manufacturer's instructions. The electropherograms showed that the RNA was not degraded or contaminated with genomic DNA. An Illumina sequencing library for Q117 and 7b4 was prepared from 1

μg of purified mRNA pooled from all replicates following the low-throughput protocol of the

Illumina TruSeq sample preparation kit. Library insert sizes were 170 bp. The libraries were

indexed and pooled and sequenced by Geneworks (Thebarton, Australia) with the Illumina

GAIIx Genome Analyzer using a single lane of paired-end 2×90 b reads (Illumina sequencing

reagents v5). The data were demultiplexed and analysed using Illumina's CASAVA 1.7

software. Differential expression between WT and 7B4 was determined following the Tophat

and Cufflinks pipeline (Trapnell et al., 2012) mapping the reads to the *Sorghum bicolor*

genome including the chloroplast and mitochondrial genomes. The alignment routine is

detailed in Supporting information Note 2.

Protein extraction

About 20 mg of lyophilised ground sugarcane leaf powder material was extracted with 50

mM HEPES-Na pH 7.3; 1mM Dithiothreitol; 0.1% Triton X-100 and 5 mM sodium ascorbate

(Brouquisse et al., 1998). Protein content was measured according to the method of Bradford

using bovine serum albumin (Promega, South Sydney, NSW, Australia) as a standard.

Data Processing and Analysis

HPLC data were processed using ChemStation (Rev B.03.02 Agilent Technologies, USA),

LC-MS/MS data using MultiQuant 2.1.1 (AB Sciex, Canada). One-way ANOVA was

performed using GraphPad Prism version 6.02 for Windows (GraphPad Software, USA). K-

means cluster analysis was performed in R (v3.0.2) (R Core Team, 2013).

Metabolic modelling

To explore the effects of PHB synthesis on ATP and NADPH demand and on the

engagement of BS and M functions, a metabolic model was developed based on that of

(Bellasio and Griffiths, 2014). The model available in Supporting information is implemented

in Excel: because all equations appear in cells, any modification is straightforward. Although

some equations used here are specific for PHB synthesis, the case in which $r_{CD}=0$

corresponds to C_4 photosynthesis as such. This version of the metabolic model does not

necessitate parameterization with gas exchange data and is therefore useful to generate

hypothetic scenarios. Based on the assumption that PHB synthesis does not disrupt the C_4

carbon concentrating mechanism (CCM), Rubisco oxygenation versus carboxylation rate was treated as a model input, expressed as:

$$r_F = \frac{V_O}{V_C}$$ 1

Carbon diversion to PHB was expressed as rate of PGA (or PYR) decarboxylation (V_D) and was incorporated in the fundamental equation of steady state assimilation, which can be expressed as:

$$A = V_C - \frac{1}{2}V_O - R_{LIGHT} - V_D$$ 2

Where A, the rate of net CO_2 flux entering stomata, integrates the rate of all CO_2 utilising and evolving processes: Rubisco carboxylation utilising CO_2 at the rate of V_C, glycolate recycling evolving $0.5CO_2$ per Rubisco oxygenation event (V_O), respiration evolving CO_2 at the rate of R_{LIGHT} and PHB synthesis evolving CO_2 at the rate V_D.

All net CO_2 entering the leaf is either converted to carbohydrates or to PHB and the stoichiometric ratio between the two is 2/3, because out of 3 carbon of PGA only 2 are stored in PHB and 1 carbon decarboxylated. This can be expressed as:

$$A = 2V_D + 3CS$$ 3

Where CS is the rate of carbohydrate (sucrose and sucrose) synthesis expressed on a triose basis.

PHB synthesis competes for PGA with the RPP cycle. The ratio of PGA allocated to PHB synthesis versus the PGA entering the RPP cycle was expressed as:

$$r_{CD} = \frac{2V_D}{3CS}$$ 4

Which reflects the stoichiometry mentioned above. Eqn 1 to 4 can form system of 4 equations and 4 unknowns, which can be used to calculate V_O, V_C, V_D and CS, inputting A, R_{LIGHT}, r_F and r_{CD}. A, R_{LIGHT} and r_F were set to C_4 realistic values of 9μmol m^{-2}·s^{-1}, 9 μmol·m^{-2}·s^{-1}, and 0.05 (Bellasio et al., 2014) while r_{CD} was varied to explore different scenarios.

The effect of allocation of PHB production to BS or M was simulated through the parameter PHB_{BS}/PHB_M which splits the total production of PHB in the two cellular compartments. Then, based on the ATP and NADPH demand of key assimilatory processes (Table S1), the rates of all other reactions reported in Table 2 was resolved. Further assumptions were $PEPCK_{MAX}$=0.05V_P (PEPCK engagement in sugarcane is minimal) PR_{BSMAX}=0.35PR_{TOT} and CS_{BSMAX}=CS_{TOT}, ratio of C_4 over-cycling [1/(1-Φ)=1.25)] (Bellasio and Griffiths, 2014).

Acknowledgements

References

Altpeter, F., Jung, J.H., Karan, R., Zale, J., Kim, J.Y., Wu, H., Dermawan, H., Pathak, B., Gretencord, R., Lui, H., Candreva, J. and Shanklin, J. (2014) Genetic Improvement of the Biofuel Feedstock Sugarcane with Intragenic, Targeted Mutagenesis and Transgenic Biotechnologies. *In Vitro Cell Dev-An* **50**, S19-S19.

Alvarez, C.E., Saigo, M., Margarit, E., Andreo, C.S. and Drincovich, M.F. (2013) Kinetics and functional diversity among the five members of the NADP-malic enzyme family from Zea mays, a C4 species. *Photosynth Res* **115**, 65-80.

Arsova, B., Hoja, U., Wimmelbacher, M., Greiner, E., Ustun, S., Melzer, M., Petersen, K., Lein, W. and Bornke, F. (2010) Plastidial thioredoxin z interacts with two fructokinase-like proteins in a thiol-dependent manner: evidence for an essential role in chloroplast development in Arabidopsis and Nicotiana benthamiana. *Plant Cell* **22**, 1498-1515.

Baena-Gonzalez, E., Rolland, F., Thevelein, J.M. and Sheen, J. (2007) A central integrator of transcription networks in plant stress and energy signalling. *Nature* **448**, 938-942.

Baier, M. and Dietz, K.J. (2005) Chloroplasts as source and target of cellular redox regulation: a discussion on chloroplast redox signals in the context of plant physiology. *J Exp Bot* **56**, 1449-1462.

Basset, G., Raymond, P., Malek, L. and Brouquisse, R. (2002) Changes in the expression and the enzymic properties of the 20S proteasome in sugar-starved maize roots. evidence for an in vivo oxidation of the proteasome. *Plant Physiol* **128**, 1149-1162.

Bellasio, C., Burgess, S.J., Griffiths, H. and Hibberd, J.M. (2014) A high throughput gas exchange screen for determining rates of photorespiration or regulation of C4 activity. *J Exp Bot* **65**, 3769-3779.

Bellasio, C. and Griffiths, H. (2014) The operation of two decarboxylases, transamination, and partitioning of C4 metabolic processes between mesophyll and bundle sheath cells allows light capture to be balanced for the maize C4 pathway. *Plant Physiol* **164**, 466-480.

Bohmert-Tatarev, K., McAvoy, S., Daughtry, S., Peoples, O.P. and Snell, K.D. (2011) High levels of bioplastic are produced in fertile transplastomic tobacco plants engineered with a synthetic operon for the production of polyhydroxybutyrate. *Plant Physiol* **155**, 1690-1708.

Bohmert, K., Balbo, I., Kopka, J., Mittendorf, V., Nawrath, C., Poirier, Y., Tischendorf, G., Trethewey, R.N. and Willmitzer, L. (2000) Transgenic Arabidopsis plants can accumulate polyhydroxybutyrate to up to 4% of their fresh weight. *Planta* **211**, 841-845.

Brouquisse, R., Gaudillere, J.P. and Raymond, P. (1998) Induction of a carbon-starvation-related proteolysis in whole maize plants submitted to Light/Dark cycles and to extended darkness. *Plant Physiol* **117**, 1281-1291.

Brouquisse, R., James, F., Pradet, A. and Raymond, P. (1992) Asparagine metabolism and nitrogen distribution during protein degradation in sugar-starved maize root tips. *Planta* **188**, 384-395.

Brouquisse, R., James, F., Raymond, P. and Pradet, A. (1991) Study of glucose starvation in excised maize root tips. *Plant Physiol* **96**, 619-626.

Chacko, A., Barker, C.J., Beagley, K.W., Hodson, M.P., Plan, M.R., Timms, P. and Huston, W.M. (2014) Increased sensitivity to tryptophan bioavailability is a positive adaptation by the human strains of Chlamydia pneumoniae. *Mol Microbiol*, **93**, 797-813.

Chen, Z.H., Jenkins, G.I. and Nimmo, H.G. (2009) pH and carbon supply control the expression of phosphoenolpyruvate carboxylase kinase genes in Arabidopsis thaliana. (vol 31, pg 1844, 2008). *Plant Cell Environ* **32**, 208-208.

Devaux, C., Baldet, P., Joubes, J., Dieuaide-Noubhani, M., Just, D., Chevalier, C. and Raymond, P. (2003) Physiological, biochemical and molecular analysis of sugar-starvation responses in tomato roots. *J Exp Bot* **54**, 1143-1151.

Di Ferdinando, M., Brunetti, C., Fini, A. and Tattini, M. (2012) Flavonoids as Antioxidants in Plants Under Abiotic Stresses. In: *Abiotic Stress Responses in Plants* (Ahmad, P. and Prasad, M.N.V. eds), pp. 159-179. Springer New York.

Dietmair, S., Hodson, M.P., Quek, L.-E., Timmins, N.E., Chrysanthopoulos, P., Jacob, S.S., Gray, P. and Nielsen, L.K. (2012) Metabolite profiling of CHO cells with different growth characteristics. *Biotechnol Bioeng* **109**, 1404-1414.

Dietmair, S., Timmins, N.E., Gray, P.P., Nielsen, L.K. and Krömer, J.O. (2010) Towards quantitative metabolomics of mammalian cells: Development of a metabolite extraction protocol. *Anal Biochem* **404**, 155-164.

Dieuaide-Noubhani, M., Canioni, P. and Raymond, P. (1997) Sugar-Starvation-Induced Changes of Carbon Metabolism in Excised Maize Root Tips. *Plant Physiol* **115**, 1505-1513.

Driever, S.M. and Kromdijk, J. (2013) Will C3 crops enhanced with the C4 CO2-concentrating mechanism live up to their full potential (yield)? *J Exp Bot* **64**, 3925-3935.

Drincovich, M.F. and Andreo, C.S. (1994) Redox Regulation of Maize Nadp-Malic Enzyme by Thiol-Disulfide Interchange - Effect of Reduced Thioredoxin on Activity. *BBA Protein Struct M* **1206**, 10-16.

Fesenko, E. and Edwards, R. (2014) Plant synthetic biology: a new platform for industrial biotechnology. *J Exp Bot* **65**, 1927-1937.

Fini, A., Brunetti, C., Di Ferdinando, M., Ferrini, F. and Tattini, M. (2011) Stress-induced flavonoid biosynthesis and the antioxidant machinery of plants. *Plant Signal Behav* **6**, 709-711.

Fukayama, H., Tamai, T., Taniguchi, Y., Sullivan, S., Miyao, M. and Nimmo, H.G. (2006) Characterization and functional analysis of phosphoenolpyruvate carboxylase kinase genes in rice. *Plant J* **47**, 258-268.

Geigenberger, P., Kolbe, A. and Tiessen, A. (2005) Redox regulation of carbon storage and partitioning in response to light and sugars. *J Exp Bot* **56**, 1469-1479.

Geiger, D.R. and Servaites, J.C. (1994) Diurnal regulation of photosynthetic carbon metabolism in C3 plants. *Annu Rev Plant Physiol Plant Mol Biol* **45**, 235-256.

Gibon, Y., Pyl, E.T., Sulpice, R., Lunn, J.E., Hohne, M., Gunther, M. and Stitt, M. (2009) Adjustment of growth, starch turnover, protein content and central metabolism to a decrease of the carbon supply when Arabidopsis is grown in very short photoperiods. *Plant Cell Environ* **32**, 859-874.

Gilkerson, J., Perez-Ruiz, J.M., Chory, J. and Callis, J. (2012) The plastid-localized pfkB-type carbohydrate kinases FRUCTOKINASE-LIKE 1 and 2 are essential for growth and development of Arabidopsis thaliana. *BMC Plant Biol* **12**, 102.

Glassop, D., Roessner, U., Bacic, A. and Bonnett, G.D. (2007) Changes in the Sugarcane Metabolome with Stem Development. Are They Related to Sucrose Accumulation? *Plant Cell Physiol* **48**, 573-584.

Hanson, J., Hanssen, M., Wiese, A., Hendriks, M.M.W.B. and Smeekens, S. (2008) The sucrose regulated transcription factor bZIP11 affects amino acid metabolism by

regulating the expression of asparagine synthetase 1 and proline dehydrogenase 2.
Plant J **53**, 935-949.

Hattersley, P.W. (1984) Characterization of C-4 type leaf anatomy in grasses (Poaceae),
mesophyll - bundle sheath area ratios. *Ann Bot-London* **53**, 163-179.

Hayakawa, T., Nakamura, T., Hattori, F., Mae, T., Ojima, K. and Yamaya, T. (1994) Cellular
localization of NADH-dependent glutamate-synthase protein in vascular bundles of
unexpanded leaf blades and young grains of rice plants. *Planta* **193**, 455-460.

James, F., Brouquisse, R., Suire, C., Pradet, A. and Raymond, P. (1996) Purification and
biochemical characterization of a vacuolar serine endopeptidase induced by glucose
starvation in maize roots. *Biochem J* **320 (Pt 1)**, 283-292.

Kajala, K., Covshoff, S., Karki, S., Woodfield, H., Tolley, B.J., Dionora, M.J.A., Mogul, R.T.,
Mabilangan, A.E., Danila, F.R., Hibberd, J.M. and Quick, W.P. (2011) Strategies for
engineering a two-celled C4 photosynthetic pathway into rice. *J Exp Bot* **62**, 3001-
3010.

Karaba, A., Dixit, S., Greco, R., Aharoni, A., Trijatmiko, K.R., Marsch-Martinez, N., Krishnan,
A., Nataraja, K.N., Udayakumar, M. and Pereira, A. (2007) Improvement of water use
efficiency in rice by expression of HARDY, an Arabidopsis drought and salt tolerance
gene. *P Natl Acad Sci USA* **104**, 15270-15275.

Kourtz, L., Dillon, K., Daughtry, S., Peoples, O.P. and Snell, K.D. (2007) Chemically inducible
expression of the PHB biosynthetic pathway in Arabidopsis. *Transgenic Res* **16**, 759-
769.

Kriechbaumer, V., Park, W.J., Piotrowski, M., Meeley, R.B., Gierl, A. and Glawischnig, E.
(2007) Maize nitrilases have a dual role in auxin homeostasis and β-cyanoalanine
hydrolysis. *J Exp Bot* **58**, 4225-4233.

Lakshmanan, P., Geijskes, R.J., Aitken, K.S., Grof, C.L.P., Bonnett, G.D. and Smith, G.R. (2005)
Sugarcane biotechnology: The challenges and opportunities. *In Vitro Cell Dev-Pl* **41**,
345-363.

Lam, H.M., Peng, S. and Coruzzi, G.M. (1994) Metabolic Regulation of the Gene Encoding
Glutamine-Dependent Asparagine Synthetase in Arabidopsis thaliana. *Plant Physiol*
106, 1347-1357.

Landell, M.G.D., Scarpari, M.S., Xavier, M.A., dos Anjos, I.A., Baptista, A.S., de Aguiar, C.L., da
Silva, D.N., Bidoia, M.A.P., Brancaliao, S.R., Bressiani, J.A., de Campos, M.F., Miguel,

P.E.M., da Silva, T.N., da Silva, V.H.P., Anjos, L.O.S. and Ogata, B.H. (2013) Residual biomass potential of commercial and pre-commercial sugarcane cultivars. *Sci Agr* **70**, 299-304.

Lea, P. and Miflin, B. (1980) Transport and metabolism of asparagine and other nitrogen compounds within the plant. In: *The biochemistry of plants* (PK, S. and E, C. eds), pp. 569-607. New York: Academic press.

Lea, P.J., Robinson, S.A. and Stewart, G.R. (1990) The enzymology and metabolism of glutamine, glutamate, and asparagine. In: *The biochemistry of plants* (PK, S. and E, C. eds), pp. 121-159. New York: Academic Press.

Magalhaes, A.C., Neyra, C.A. and Hageman, R.H. (1974) Nitrite assimilation and amino nitrogen synthesis in isolated spinach chloroplasts. *Plant Physiol* **53**, 411-415.

Matsuoka, M., Kyozuka, J., Shimamoto, K. and Kano-Murakami, Y. (1994) The promoters of two carboxylases in a C4 plant (maize) direct cell-specific, light-regulated expression in a C3 plant (rice). *Plant J* **6**, 311-319.

McQualter, R.B., Petrasovits, L.A., Gebbie, L.K., Schweitzer, D., Blackman, D.M., Riches, J.D., Snell, K.D., Brumbley, S.M. and Nielsen, L.K. (2014a) The use of an acetoacetyl-CoA synthase in place of a β-ketothiolase enhances poly-3-hydroxybutyrate production in sugarcane mesophyll cells. . *Plant Biotechnol J*, doi: 10.1111/pbi.12298.

McQualter, R.B., Somleva, M.N., Gebbie, L.K., Xuemei, L., Petrasovits, L.A., Snell, K.D., Nielsen, L.K. and Brumbley, S.M. (2014b) Factors affecting polyhydroxybutyrate accumulation in mesophyll cells of C4 grasses. *BMC Biotechnol* **14**, doi:10.1186/1472-6750-1114-1183.

Michalska, J., Zauber, H., Buchanan, B.B., Cejudo, F.J. and Geigenberger, P. (2009) NTRC links built-in thioredoxin to light and sucrose in regulating starch synthesis in chloroplasts and amyloplasts. *Proc Natl Acad Sci U S A* **106**, 9908-9913.

Ming, R., Moore, P.H., Wu, K.K., D'Hont, A., Glaszmann, J.C., Tew, T.L., Mirkov, T.E., da Silva, J., Jifon, J., Rai, M., Schnell, R.J., Brumbley, S.M., Lakshmanan, P., Comstock, J.C. and Paterson, A.H. (2006) Sugarcane Improvement through Breeding and Biotechnology. *Pl Bred Re* **27**, 15-118.

Morandini, P. (2013) Control limits for accumulation of plant metabolites: brute force is no substitute for understanding. *Plant Biotechnol J* **11**, 253-267.

Nawrath, C., Poirier, Y. and Somerville, C. (1994) Targeting of the polyhydroxybutyrate
    biosynthetic pathway to the plastids of *Arabidopsis thaliana* results in high levels of
    polymer accumulation. *Proc Natl Acad Sci U S A* **91**, 12760-12764.

Nel, S. (2010) The potential of biotechnology in the sugarcane industry: Are you ready for
    the next evolution? *Int Sugar J* **112**, 11-16.

Nielsen, T.H., Rung, J.H. and Villadsen, D. (2004) Fructose-2,6-bisphosphate: a traffic signal
    in plant metabolism. *Trends Plant Sci* **9**, 556-563.

Okamoto, M., Vidmar, J.J. and Glass, A.D.M. (2003) Regulation of NRT1 and NRT2 Gene
    Families of Arabidopsis thaliana: Responses to Nitrate Provision. *Plant Cell Physiol*
    44, 304-317.

Orsel, M., Eulenburg, K., Krapp, A. and Daniel-Vedele, F. (2004) Disruption of the nitrate
    transporter genes AtNRT2.1 and AtNRT2.2 restricts growth at low external nitrate
    concentration. *Planta* **219**, 714-721.

Pan, Y.B. (2012) Biotechnology: Impact on Sugarcane Agriculture and Industry. *Sugar Tech*
    14, 1-2.

Park, W.J., Kriechbaumer, V., Müller, A., Piotrowski, M., Meeley, R.B., Gierl, A. and
    Glawischnig, E. (2003) The Nitrilase ZmNIT2 Converts Indole-3-Acetonitrile to Indole-
    3-Acetic Acid. *Plant Physiol* **133**, 794-802.

Petrasovits, L.A., McQualter, R.B., Gebbie, L.K., Blackman, D.M., Nielsen, L.K. and Brumbley,
    S.M. (2013) Chemical inhibition of acetyl coenzyme A carboxylase as a strategy to
    increase polyhydroxybutyrate yields in transgenic sugarcane. *Plant Biotechnol J* **11**,
    1146-1151.

Petrasovits, L.A., Purnell, M.P., Nielsen, L.K. and Brumbley, S.M. (2007) Production of
    polyhydroxybutyrate in sugarcane. *Plant Biotechnol J* **5**, 162-172.

Petrasovits, L.A., Zhao, L., McQualter, R.B., Snell, K.D., Somleva, M.N., Patterson, N.A.,
    Nielsen, L.K. and Brumbley, S.M. (2012) Enhanced polyhydroxybutyrate production
    in transgenic sugarcane. *Plant Biotechnol J* **10**, 569-578.

Philip, S., Keshavarz, T. and Roy, I. (2007) Polyhydroxyalkanoates: biodegradable polymers
    with a range of applications. *J Chem Technol Biot* **82**, 233-247.

Pick, T.R., Brautigam, A., Schluter, U., Denton, A.K., Colmsee, C., Scholz, U., Fahnenstich, H.,
    Pieruschka, R., Rascher, U., Sonnewald, U. and Weber, A.P. (2011) Systems analysis

of a maize leaf developmental gradient redefines the current C4 model and provides

candidates for regulation. *Plant Cell* **23**, 4208-4220.

Poirier, Y., Dennis, D.E., Klomparens, K. and Somerville, C. (1992) Polyhydroxybutyrate, a

Biodegradable Thermoplastic, Produced in Transgenic Plants. *Science* **256**, 520-523.

Poirier, Y. and Gruys, K.J. (2001) Production of polyhydroxyalkanoates in transgenic plants.

In: *Biopolymer* (Doi, Y. and Steinbuchel, A. eds), pp. 401-435. Berlin: Wiley-VHC.

Purnell, M.P., Petrasovits, L.A., Nielsen, L.K. and Brumbley, S.M. (2007) Spatio-temporal

characterization of polyhydroxybutyrate accumulation in sugarcane. *Plant Biotechnol*

J **5**, 173-184.

R Core Team (2013) R: A language and environment for statistical computing, Vienna,

Austria: R Foundation for Statistical Computing. ISBN 3-900051-07-0, http://www.R-

project.org/.

Rae, A.L., Casu, R.E., Perroux, J.M., Jackson, M.A. and Grof, C.P.L. (2011) A soluble acid

invertase is directed to the vacuole by a signal anchor mechanism. *J Plant Physiol*

168, 983-989.

Reddy, A.R. and Das, V.S.R. (1987) Modulation of Sucrose Content by Fructose 2,6-

Bisphosphate during Photosynthesis in Rice Leaves Growing at Different Light

Intensities. *J Exp Biol* **38**, 828-833.

Rossato, L., Lainé, P. and Ourry, A. (2001) Nitrogen storage and remobilization in Brassica

napus L. during the growth cycle: nitrogen fluxes within the plant and changes in

soluble protein patterns. *J Exp Bot* **52**, 1655-1663.

Sage, R.F., Peixoto, M.M. and Sage, T.L. (2013) Photosynthesis in Sugarcane. In: *Sugarcane:*

Physiology, Biochemistry, and Functional Biology (Moore, P.H. and Botha, F.C. eds),

pp. 121-154. Chichester, UK: John Wiley & Sons Ltd.

Sakakibara, H., Kawabata, S., Hase, T. and Sugiyama, T. (1992) Differential Effects of Nitrate

and Light on the Expression of Glutamine Synthetases and Ferredoxin-Dependent

Glutamate Synthase in Maize. *Plant Cell Physiol* **33**, 1193-1198.

Saruul, P., Srienc, F., Somers, D.A. and Samac, D.A. (2002) Production of a biodegradable

plastic polymer, poly-b-hydroxybutyrate, in transgenic alfalfa. *Crop Sci* **42**, 919-927.

Schluter, U., Colmsee, C., Scholz, U., Brautigam, A., Weber, A.P., Zellerhoff, N., Bucher, M.,

Fahnenstich, H. and Sonnewald, U. (2013) Adaptation of maize source leaf

metabolism to stress related disturbances in carbon, nitrogen and phosphorus balance. *BMC Genomics* **14**, 442.

Schluter, U., Mascher, M., Colmsee, C., Scholz, U., Brautigam, A., Fahnenstich, H. and Sonnewald, U. (2012) Maize source leaf adaptation to nitrogen deficiency affects not only nitrogen and carbon metabolism but also control of phosphate homeostasis. *Plant Physiol* **160**, 1384-1406.

Shenton, M., Fontaine, V., Hartwell, J., Marsh, J.T., Jenkins, G.I. and Nimmo, H.G. (2006) Distinct patterns of control and expression amongst members of the PEP carboxylase kinase gene family in C4 plants. *Plant J* **48**, 45-53.

Sieciechowicz, K.A., Joy, K.W. and Ireland, R.J. (1988) The metabolism of asparagine in plants. *Phytochemistry* **27**, 663-671.

Sluiter, A. and Sluiter, J. (2005) Determination of starch in solid biomass samples by HPLC. *NREL Laboratory Analytical Procedure.< http://devafdc. nrel. gov/pdfs/9360. pdf*.

Smolke, C.D. and Silver, P.A. (2011) Informing Biological Design by Integration of Systems and Synthetic Biology. *Cell* **144**, 855-859.

Somleva, M.N., Chinnapen, H., Ali, A., Snell, K.D., Peoples, O.P., Patterson, N., Tang, J. and Bohmert-Tatarev, K. (2012) Increasing carbon flow for polyhydroxybutyrate production in biomass crops. US Patent Application.

Somleva, M.N., Peoples, O.P. and Snell, K.D. (2013) PHA bioplastics, biochemicals, and energy from crops. *Plant Biotechnol J* **11**, 233-252.

Somleva, M.N., Snell, K.D., Beaulieu, J.J., Peoples, O.P., Garrison, B.R. and Patterson, N.A. (2008) Production of polyhydroxybutyrate in switchgrass, a value-added co-product in an important lignocellulosic biomass crop. *Plant Biotechnol J* **6**, 663-678.

Srienc, F., Arnold, B. and Bailey, J.E. (1984) Characterization of intracellular accumulation of poly-beta-hydroxybutyrate (PHB) in individual cells of Alcaligenes eutrophus H16 by flow cytometry. *Biotechnol Bioeng* **26**, 982-987.

Sullivan, T.D., Christensen, A.H. and Quail, P.H. (1989) Isolation and characterization of a maize chlorophyll a/b binding protein gene that produces high levels of mRNA in the dark. *Mol Gen Genet* **215**, 431-440.

Thormahlen, I., Ruber, J., von Roepenack-Lahaye, E., Ehrlich, S.M., Massot, V., Hummer, C., Tezycka, J., Issakidis-Bourguet, E. and Geigenberger, P. (2013) Inactivation of thioredoxin f1 leads to decreased light activation of ADP-glucose pyrophosphorylase

and altered diurnal starch turnover in leaves of Arabidopsis plants. *Plant Cell Environ* **36**, 16-29.

Tilbrook, K., Gebbie, L., Schenk, P.M., Poirier, Y. and Brumbley, S.M. (2011) Peroxisomal polyhydroxyalkanoate biosynthesis is a promising strategy for bioplastic production in high biomass crops. *Plant Biotechnol J* **9**, 958-969.

Tilbrook, K., Poirier, Y., Gebbie, L., Schenk, P.M., McQualter, R.B. and Brumbley, S.M. (2014) Reduced peroxisomal citrate synthase activity increases substrate availability for polyhydroxyalkanoate biosynthesis in plant peroxisomes. *Plant Biotechnol J* **12**, 1044-1052.

Trapnell, C., Roberts, A., Goff, L., Pertea, G., Kim, D., Kelley, D.R., Pimentel, H., Salzberg, S.L., Rinn, J.L. and Pachter, L. (2012) Differential gene and transcript expression analysis of RNA-seq experiments with TopHat and Cufflinks. *Nat. Protocols* **7**, 562-578.

Valerio, C., Costa, A., Marri, L., Issakidis-Bourguet, E., Pupillo, P., Trost, P. and Sparla, F. (2011) Thioredoxin-regulated beta-amylase (BAM1) triggers diurnal starch degradation in guard cells, and in mesophyll cells under osmotic stress. *J Exp Bot* **62**, 545-555.

Van Norman, J.M. and Benfey, P.N. (2009) Arabidopsis thaliana as a model organism in systems biology. *Wiley Interdisc Rev Syst Biol Med* **1**, 372-379.

Varshney, R.K., Bansal, K.C., Aggarwal, P.K., Datta, S.K. and Craufurd, P.Q. (2011) Agricultural biotechnology for crop improvement in a variable climate: hope or hype? *Trends Plant Sci* **16**, 363-371.

von Caemmerer, S., Quick, W.P. and Furbank, R.T. (2012) The development of C4 rice: current progress and future challenges. *Science* **336**, 1671-1672.

Watanabe, S., Sakai, T., Goto, S., Yaginuma, T., Hayakawa, T. and Yamaya, T. (1996) Expression of NADH-Dependent Glutamate Synthase in Response to the Supply of Nitrogen in Rice Cells in Suspension Culture. *Plant and Cell Physiology* **37**, 1034-1037.

Weise, S.E., van Wijk, K.J. and Sharkey, T.D. (2011) The role of transitory starch in C(3), CAM, and C(4) metabolism and opportunities for engineering leaf starch accumulation. *J Exp Bot* **62**, 3109-3118.

Zhu, X.G., Shan, L.L., Wang, Y. and Quick, W.P. (2010) C4 Rice - an Ideal Arena for Systems Biology Research. *J Integr Plant Biol* **52**, 762-770.

Zurbriggen, M.D., Moor, A. and Weber, W. (2012) Plant and bacterial systems biology as platform for plant synthetic bio(techno)logy. *J Biotechnol* **160**, 80-90.

Tables

Table 1: Sugarcane genes from central carbon metabolism which showed significant (p value and q value both < 0.05) differential expression between WT and PHB-producer.

EC number	function	Equivalent Sorghum gene	WT (fpkm)	7b4 (fpkm*)	log$_2$ (fold change)
n/a	MFS transporter, NNP family, nitrate/nitrite transporter	Sb03g032310	15.9371	1.11527	-3.84
3.2.1.26	Beta-fructofuranosidase -soluble acid invertase vacuolar	Sb04g000620	85.6464	7.18532	-3.58
2.7.11.1	Phosphoenolpyruvate carboxylase kinase 1	Sb04g036570	48.7546	4.86261	-3.33
2.4.1.21	Starch synthase III-1a	Sb07g005400	2.58404	0.34752	-2.89
1.1.1.40	NADP-ME cytoplasmic	Sb03g034280	45.7206	8.69798	-2.39
3.5.5.1	Nitrilase / nitrile aminohydrolase	Sb04g026940	121.798	25.2263	-2.27
5.4.2.2	Phosphoglucomutase chloroplastic	Sb03g028080	24.7318	138.489	2.49
6.3.5.4	Asparagine synthetase [glutamine-hydrolyzing] chloroplastic	Sb05g000440	40.1626	260.054	2.69
1.4.1.14/ 1.4.1.13	glutamate synthase (NADPH/NADH) chloroplastic	Sb09g027910	0.510637	3.33429	2.71
4.3.1.24	Phenylalanine ammonia-lyase	Sb06g022750	9.97267	67.2266	2.75
n/a	fructokinase-like chloroplastic	Sb01g015030	2.16637	14.8773	2.78
2..4.1.13	sucrose synthase SUS1	Sb01g033060	15.2643	120.981	2.99
3.2.1.26	Beta-fructofuranosidase 1	Sb06g023760	1.00096	11.3446	3.50
3.2.1.2	Beta amylase 5 cytosolic	Sb02g035600	0.822546	14.6832	4.16

*FPKM – fragments per kilobase of transcript per million mapped fragments

Table 2. Equations for the reaction rates of C_4 assimilation and PHB production.

Equations for fluxes between BS and M are reported in Supporting information Table S4.

Process	Symbol	Reaction rate	Eqn	Localization	Notes
PGA reduction tot	PR_{TOT}	$2V_C + \frac{3}{2}V_O - \frac{1}{3}R_{LIGHT} - V_D$	5	BS and M	2 V_C is the PGA produced by the carboxylating activity of Rubisco; V_O is the PGA produced by the oxygenating activity of Rubisco; 0.5 V_O is the PGA regenerated by the photorespiratory cycle; 1/3 is the stoichiometric conversion between respiration (expressed per CO_2), which in this model is supplied by PGA, and PR (expressed per triose) and finally, PYR decarboxylation reduces the rate of PGA reduction.
RuP phosphorylation	RuP_{phosp}	$V_c + V_o$	6	BS	At steady state the rate of RuBP produced through phosphorylation equals the rate of RuBP consumed through Rubisco carboxylating activity (V_C), together with oxygenating activity (V_O).
DHAP entering RPP	$DHAP_{RPP}$	$\frac{5}{3}RuP_{phosp}$	7	BS	Since carbohydrates are considered the final products of photosynthesis and are synthsized using DHAP as a precursor, the RPP supplies solely RuP regeneration. 5/3 converts the stoichiometry of RuP (C_5) to the stoichiometry of $DHAP$ (C_3).
Carbohydrate synthesis tot	CS_{TOT}	$PR_{TOT} - DHAP_{RPP}$	8	BS and M	The total carbohydrate synthesis corresponds to the total PGA reduced minus the triose required for RuBP regeneration ($DHAP_{RPP}$).
NADPH demand tot	$NADPH_{TOT}$	$PR_{TOT} + \frac{1}{2}V_O - \frac{1}{2}V_D$	9	BS and M	PGA reduction consumes 1 NADPH per triose. In the photorespiratory glycolate regeneration (per glycolate) in total 0.5 NADPH is consumed per glycolate (at a rate equivalent to V_O, Supplementary Table S3), while PHB synthesis produces 0.5 NADPH per pyruvate decarboxylation event (-0.5V_D).
ATP demand tot	ATP_{BS} + ATP_M	$PR_{TOT} + RuP_{phosp} + V_O + \frac{1}{2}CS_{TOT} + PEPCK + 2PPDK - V_D$	10	BS and M	The total ATP demand is brought about by PGA reduction (corresponding to PR), RuBP regeneration (corresponding to RuP_{phosp}), glycolate recycling (corresponding to V_O), carbohydrate synthesis (corresponding to CS), PEP regeneration (1 ATP per PEPCK catalytic event or 2 ATP per PPDK catalytic event) and by PYR decarboxylation which actually produces 1 ATP per V_D.
ATP demand in BS	ATP_{BS}	$PR_{BS} + V_C + 2V_O + \frac{1}{2}CS_{BS} + PEPCK - V_{DBS}$	11	BS	The ATP demand in BS is brought about by PGA reduction, RuBP regeneration, glycolate recycling, carbohydrate synthesis and PEPCK.
ATP demand in M	ATP_M	$2PPDK + \frac{1}{2}CS_M + PR_M - V_{DM}$	12	M	The ATP demand in M is brought about by PGA reduction, carbohydrate synthesis and PPDK.
NADPH demand in BS	$NADPH_{BS}$	$PR_{BS} + \frac{1}{2}V_O - \frac{1}{2}V_{DBS}$	13	BS	The NADPH demand in BS is brought about by PGA reduction and glycolate recycling.
NADPH demand in M	$NADPH_M$	$NADPH_{TOT} - NADPH_{BS}$	14		NADPH demand in M and BS are complementary
PGA reduction M	PR_M	$PR_{TOT} - PR_{BS}$	15	M	PGA reduction is a process shared by BS and M.
Pyruvate phosphate dikinase	$PPDK$	$V_P - PEPCK$	16	M	The PEP regenerated by PEPCK in BS diffuses to M and reduces the requirement of PEP regenerated by PPDK in M.
PEP regeneration tot	-	V_P	17	BS and M	PEP regeneration rate equals PEP consumption rate V_P at steady state. PEP can be regenerated either by PPDK (mainly in M, but active also in BS) or by PEPCK in BS. PPDK activity was assumed to be zero in BS. V_P was calculated by assuming a realistic rate of C_4 overcycling (see note to Eqn 18).
PEPC rate	V_P	$\frac{A + R_M}{1 - \Phi}$	18	M	Under the assumption that PHB synthesis does not disrupt the CCM, V_P was estimated from the rate of overcycling 1/(1-Φ), where $Φ$ is BS leakiness, assumed 0.2.
Transamination	T	$V_P - MDH_M$	19	BS and M	T has the function of balancing NADPH supply and demand.
NADPH supply to BS	-	MDH_M	20	BS	The NADPH supply to BS corresponds to the NADPH used to reduce OAA to MAL in M, and not to the rate of MAL decarboxylation in BS, which depends on T, $PEPCK$ and MDH_{BS}.
MDH activity in M	MDH_M	$PR_{BS} + \frac{1}{2}V_O - \frac{1}{2}V_{DBS}$	21	M	MDH activity supplies the NADPH demand in BS. Eqn 21 was derived by combining Eqn 13 and 20.

Figures

Figure 1: Schematic of C_4 assimilation and PHB production in sugarcane: Rubisco carboxylation, the RPP pathway, carbohydrate synthesis, respiration, glyoxylate recycling, PHB biosynthesis with their ATP and NADPH requirements. Pyr – pyruvate; PEP – phosphoenolpyruvate; PPDK – Pyruvate, phosphate dikinase; MDH – malate dehydrogenase; PEPCK – phosphoenolpyruvate carboxykinase; OAA – oxaloacetic acid; Mal – malate; ME – NADPH dependent malic enzyme; Asp – aspartate; Ala – alanine; T – transamination; Carb – carbohydrates; PHB – polyhydroxybutyrate; DHAP – Dihydroxyacetone phosphate; PGA – 3-phosphoglycerate; PGla – 2-phosphoglycolate; RuBP – ribulose-1,5-bisphosphate; RuP - ribulose 5-phosphate. Enzyme reaction rates (in bold) are mathematically expressed in Table 2.

Figure 2. Assimilation rate in transgenic PHB-producing and WT Q117 sugarcane. Sugarcane lines are shown in rank order of PHB production from lowest to highest (left to right). Typical PHB content in these plants are (on dry weight): Q117, 0 g/100g; TA4, 0.45±0.02 g/100g; 4F1, 1.21±0.24 g/100g; 8C8, 1.3±0.11 g/100g; 7C3, 3.11±0.31 g/100g. Error bars show standard deviation. *Significantly different from WT (P<0.05). TA4, 8C8, 7C3, n=3; WT, n=5; 4F1, n=6).

Figure 3. Carbon/nitrogen balance and protein content in WT and PHB-producing sugarcane leaves. (a) Total carbon. (b) Total nitrogen. (c) Carbon/nitrogen ratio. (d) Protein content. Mean±SD is shown. For carbon and nitrogen, n=2; for protein, n=21.

Figure 4: Metabolite abundance in the leaves of WT and PHB-producing sugarcane 7B4 and 7C3 across a 12 hour light/12 hour dark diurnal cycle. Samples were collected every four hours commencing at first light, n=3. Grey shading shows dark period. Abbreviations and statistic clustering are reported in supporting information Note1 and Figure S1 respectively.

Figure 5: Changes in metabolic processes in response to increasing allocation of carbon to PHB synthesis at the expense of carbohydrate synthesis (r_{CD}) and with respect to PHB partitioning between M and BS cells (V_{DBS}/V_D). (a) Total ATP demand relative to gross assimilation. (b) Total NADPH demand relative to gross assimilation. (c) ATP demand in BS relative to ATP demand in M. (d) NADPH demand in BS relative to NADPH demand in M. (e) Transamination rate. (f) Aspartate decarboxylation rate relative to Malate decarboxylation rate. V_D–PHB synthesis expressed as rate of PGA decarboxylation; V_{DBS}–PHB synthesis in BS; r_{CD}–relative distribution of PGA (PHB/carbohydrates).

1
2
3
4
5
6
7
8
9
10
11
12
13
14
15
16
17
18
19
20
21
22
23
24
25
26
27
28
29
30
31
32
33
34
35
36
37
38
39
40
41
42
43
44
45
46
47
48
49
50
51
52
53
54
55
56
57
58
59
60

Figure 6: TEM of polyhydroxybutyrate granules inside the BS chloroplasts of a sugarcane leaf from a low PHB producer. The image shows chloroplast structure containing intact grana and starch granules contrasting with areas of disrupted grana where PHB granules are present. This image was generated as part of the Petrasovits et al. (2012) study but not published at the time. BS – bundle sheath cell; M – mesophyll cell; PHB – polyhydroxybutyrate.

Figure 1. Schematic of C_4 assimilation and PHB production in sugarcane: Rubisco carboxylation, the RPP pathway, carbohydrate synthesis, respiration, glyoxylate recycling, PHB biosynthesis with their ATP and NADPH requirements. Pyr – pyruvate; PEP – phosphoenolpyruvate; PPDK – Pyruvate, phosphate dikinase; MDH – malate dehydrogenase; PEPCK – phosphoenolpyruvate carboxykinase; OAA – oxaloacetic acid; Mal – malate; ME – NADPH dependent malic enzyme; Asp – aspartate; Ala – alanine; T – transamination; Carb – carbohydrates; PHB – polyhydroxybutyrate; DHAP – Dihydroxyacetone phosphate; PGA – 3-phosphoglycerate; PGla – 2-phosphoglycolate; RuBP – ribulose-1,5-bisphosphate; RuP - ribulose 5-phosphate. Enzyme reaction rates (in bold) are mathematically expressed in Table 2.
128x98mm (300 x 300 DPI)

1
2
3
4
5
6
7
8
9
10
11
12
13
14
15
16
17
18
19
20
21
22
23
24
25
26
27
28
29
30
31
32
33
34
35
36
37
38
39
40
41
42
43
44
45
46
47
48
49
50
51
52
53
54
55
56
57
58
59
60

Figure 2. Assimilation rate in transgenic PHB-producing and WT Q117 sugarcane. Sugarcane lines are shown in rank order of PHB production from lowest to highest (left to right). Typical PHB content in these plants are (on dry weight): Q117, 0 g/100g; TA4, 0.45±0.02 g/100g; 4F1, 1.21±0.24 g/100g; 8C8, 1.3±0.11 g/100g; 7C3, 3.11±0.31 g/100g. Error bars show standard deviation. *Significantly different from WT ($P<0.05$). TA4, 8C8, 7C3, n=3; WT, n=5; 4F1, n=6). 69x54mm (300 x 300 DPI)
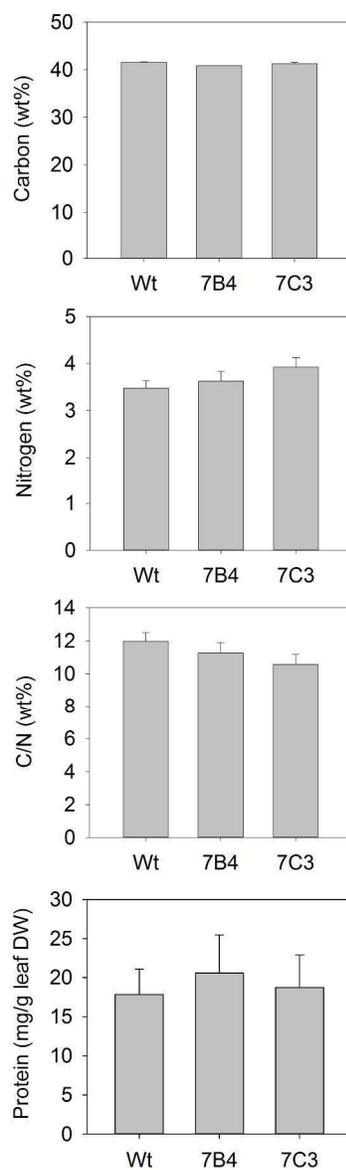
1
2
3
4
5
6
7
8
9
10
11
12
13
14
15
16
17
18
19
20
21
22
23
24
25
26
27
28
29
30
31
32
33
34
35
36
37
38
39
40
41
42
43
44
45
46
47
48
49
50
51
52
53
54
55
56
57
58
59
60

Figure 3. Carbon/nitrogen balance and protein content in WT and PHB-producing sugarcane leaves. (a) Total carbon. (b) Total nitrogen. (c) Carbon/nitrogen ratio. (d) Protein content. Mean±SD is shown. For carbon and nitrogen, n=2; for protein, n=21.
203x650mm (300 x 300 DPI)
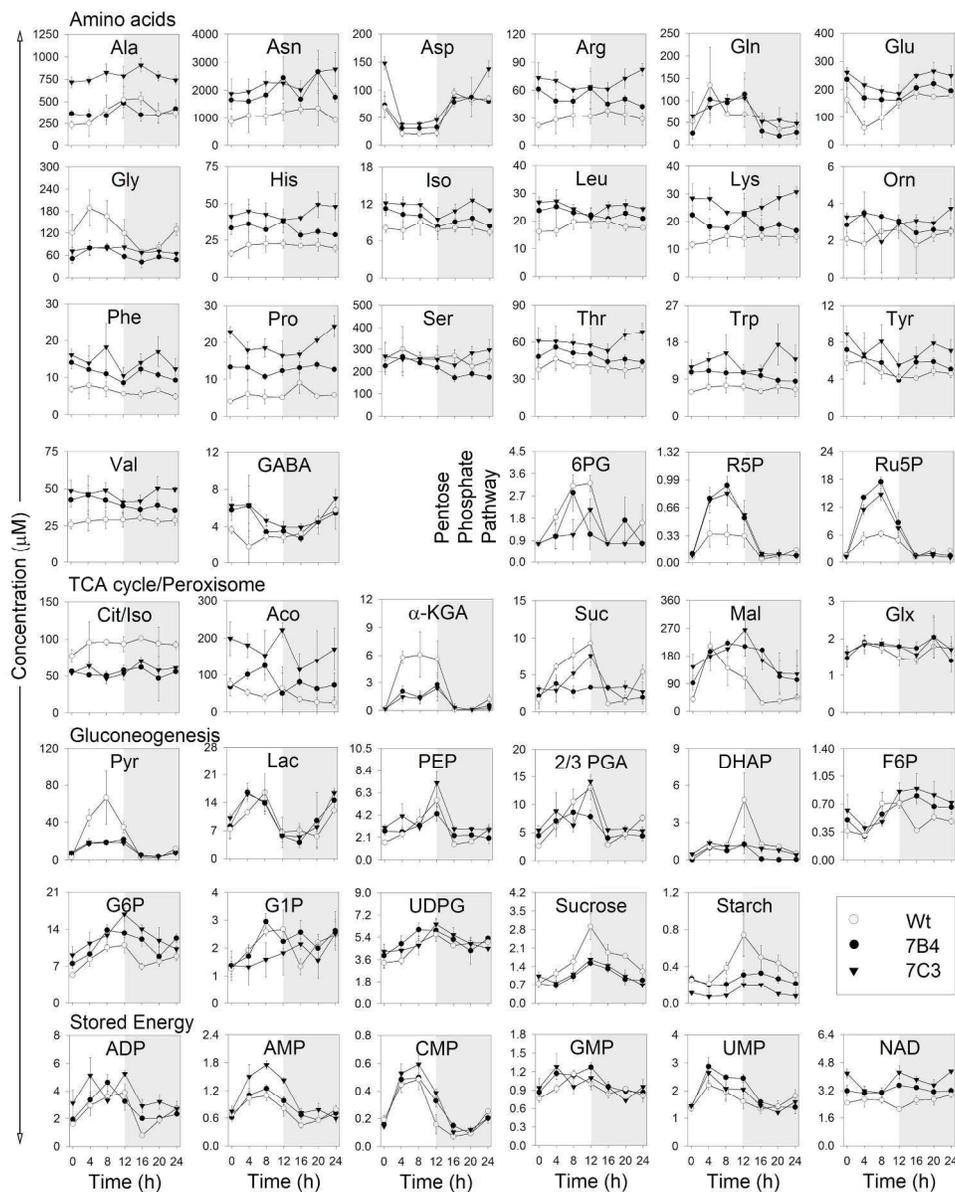
Figure 4. Metabolite abundance in the leaves of WT and PHB-producing sugarcane 7B4 and 7C3 across a 12 hour light/12 hour dark diurnal cycle. Samples were collected every four hours commencing at first light, n=3. Grey shading shows dark period. Abbreviations and statistic clustering are reported in supporting information Note1 and Figure S1 respectively.

214x265mm (300 x 300 DPI)

Figure 5. Changes in metabolic processes in response to increasing allocation of carbon to PHB synthesis at the expense of carbohydrate synthesis (rCD) and with respect to PHB partitioning between M and BS cells (VDBS/VD). (a) Total ATP demand relative to gross assimilation. (b) Total NADPH demand relative to gross assimilation. (c) ATP demand in BS relative to ATP demand in M. (d) NADPH demand in BS relative to NADPH demand in M. (e) Transamination rate. (f) Aspartate decarboxylation rate relative to Malate decarboxylation rate. VD–PHB synthesis expressed as rate of PGA decarboxylation; VDBS–PHB synthesis in BS; rCD–relative distribution of PGA (PHB/carbohydrates).
190x248mm (300 x 300 DPI)
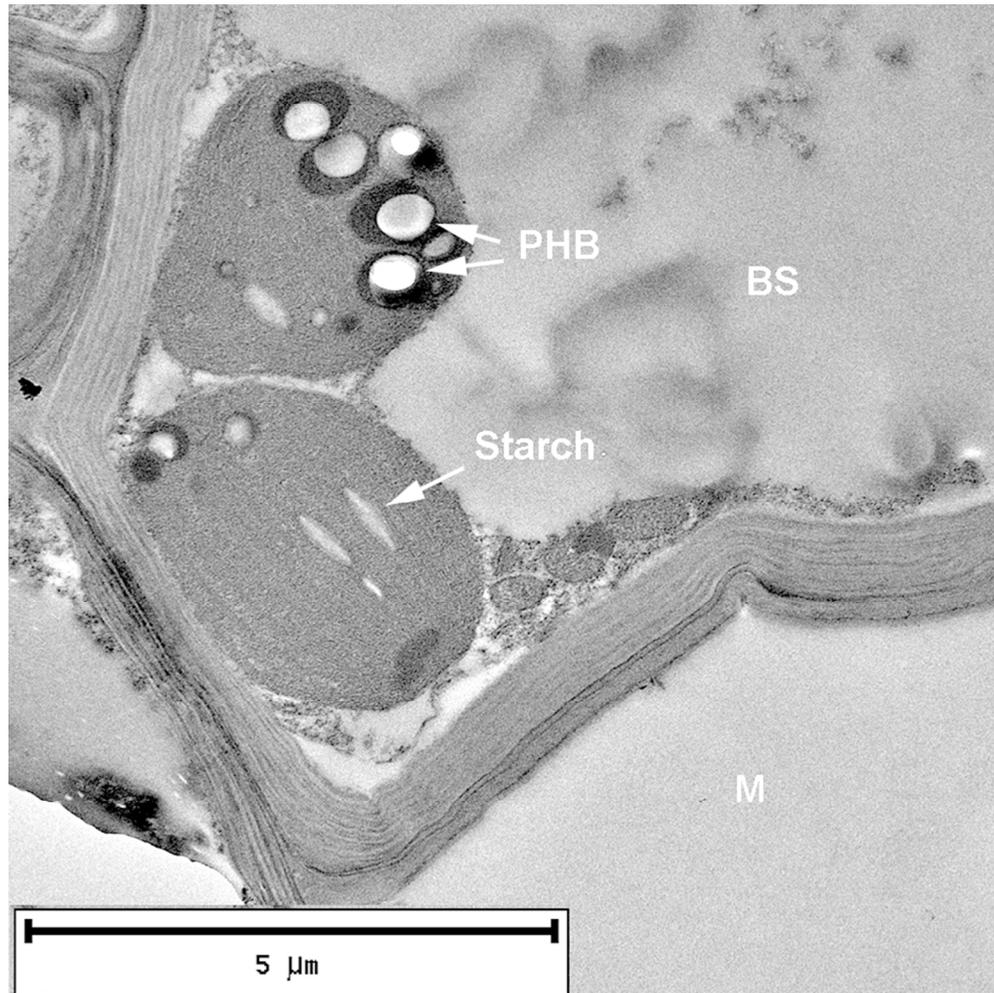
Figure 6. TEM of polyhydroxybutyrate granules inside the BS chloroplasts of a sugarcane leaf from a low PHB producer. The image shows chloroplast structure containing intact grana and starch granules contrasting with areas of disrupted grana where PHB granules are present. This image was generated as part of the Petrasovits et al. (2012) study but not published at the time. BS – bundle sheath cell; M – mesophyll cell; PHB – polyhydroxybutyrate.
80x80mm (300 x 300 DPI)